Supplement of Atmos. Chem. Phys., 18, 17307–17323, 2018
https://doi.org/10.5194/acp-18-17307-2018-supplement

Supplement of

The underappreciated role of nonvolatile cations in aerosol ammonium-sulfate molar ratios

Hongyu Guo et al.

Correspondence to: Rodney J. Weber (rweber@eas.gatech.edu) and Athanasios Nenes (athanasios.nenes@gatech.edu)

S1. Differences in molar ratio (*R*) observations between SOAS, SEAECH, and CSN

Table S1. Comparisons of observed $PM_{2.5}$ ions and molar ratio between SOAS, SEARCH, and CSN ground sampling sites for the 11-23 June 2013 period (Fig. 1 in the main text). Since CSN (Chemical Speciation Network) doesn't have a site at CTR to be directly compared to SOAS and SEARCH, the two closest sites at Birmingham (BHM) and Montgomery (MTG) are used. The most direct comparison is between Birmingham SEARCH and CSN data. Means are shown with standard deviations.

Network	SOAS	SOAS	SEARCH	SEARCH	CSN	CSN
Site location	CTR	CTR	CTR	BHM	BHM	MTG
Site coordinate	32.90289, −87.24968	32.90289, −87.24968	32.90289, −87.24968	33.55302, −86.81485	33.49972, −86.92417	32.41281, −86.26339
Method	PILS-IC	MARGA(-IC)	Teflon filter(-IC)	Teflon filter(-IC)	Nylon filter(-IC)	Nylon filter(-IC)
NH_4^+, μg m^{-3}	0.64 ± 0.22	0.79 ± 0.22	0.63 ± 0.13[*]	0.69 ± 0.20[*]	0.24 ± 0.14	0.25 ± 0.19
SO_4^{2-}, μg m^{-3}	2.06 ± 0.68	2.38 ± 0.66	2.16 ± 0.44	2.23 ± 0.51	1.69 ± 0.40	1.46 ± 0.84
Na^+, μg m^{-3}	0.07 ± 0.09	0.09 ± 0.10	0.06 ± 0.04	0.05 ± 0.04	0.13 ± 0.06	0.10 ± 0.04
R	**1.70 ± 0.23**	**1.78 ± 0.18**	**1.57 ± 0.11**	**1.64 ± 0.14**	**0.70 ± 0.36**	**0.75 ± 0.42**
Data points	229	229	13	4	5	3
Notes on data	Hourly data	Hourly data	Daily data; every day	Daily data; every three days (6/12-6/21)	Daily data; every three days (6/9-6/24)	Daily data; every six days (6/9-6/21)
Reference	(Guo et al., 2015)	(Allen et al., 2015)	(Edgerton et al., 2005; Hidy et al., 2014)		(Solomon et al., 2014)	

[*] SEARCH NH_4^+ was measured by automated colorimetry.

Table S2. Comparisons of observed $PM_{2.5}$ ions and molar ratio between SEARCH and CSN ground sampling sites for the year of 2013.

Network	SEARCH	SEARCH	CSN	CSN
Site location	CTR	BHM	BHM	MTG
Site coordinate	32.90289, −87.24968	33.55302, −86.81485	33.49972, −86.92417	32.41281, −86.26339
Method	Teflon filter(-IC)	Teflon filter(-IC)	Nylon filter(-IC)	Nylon filter(-IC)
NH_4^+, μg m^{-3}	0.55 ± 0.28[*]	0.72 ± 0.31[*]	0.48 ± 0.34	0.41 ± 0.29
SO_4^{2-}, μg m^{-3}	1.71 ± 0.89	1.96 ± 0.90	1.91 ± 0.99	1.65 ± 0.89
Na^+, μg m^{-3}	0.05 ± 0.05	0.05 ± 0.05	0.13 ± 0.30	0.10 ± 0.08
R	**1.75 ± 0.28**	**2.05 ± 0.05**	**1.26 ± 0.59**	**1.24 ± 0.59**
Data points	154	111	93	61
Notes on data	Daily data; every three days	Daily data; every three days	Daily data; every three days	Daily data; every six days
Reference	(Edgerton et al., 2005; Hidy et al., 2014)		(Solomon et al., 2014)	

[*] SEARCH NH_4^+ was measured by automated colorimetry.

S2. Relative fractions of SO_4^{2-} and HSO_4^- for SOAS fine particles

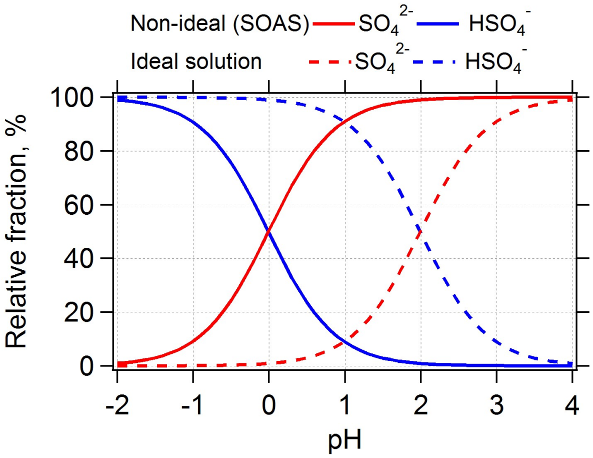

Fig. S1. Relative fractions of SO_4^{2-} (red) and HSO_4^- (blue) calculated based on ideal solutions (all activity coefficients equal one) and the SOAS non-ideal conditions. The average activity coefficients of $\gamma_{SO_4^{2-}}/\gamma_{HSO_4^-} = 0.01$ are predicted by ISORROPIA for the SOAS fine particles. $\gamma_{H^+} = 1$ is assumed; a smaller γ_{H^+} shifts the red and blue curves towards the left, increasing SO_4^{2-} relative fraction at a given pH. The dissociation constant of HSO_4^- is 1.015×10^{-2} mol kg^{-1} at 298.15 K (Fountoukis and Nenes, 2007).

S3. Comparison of PILS NVCs to MARGA NVCs

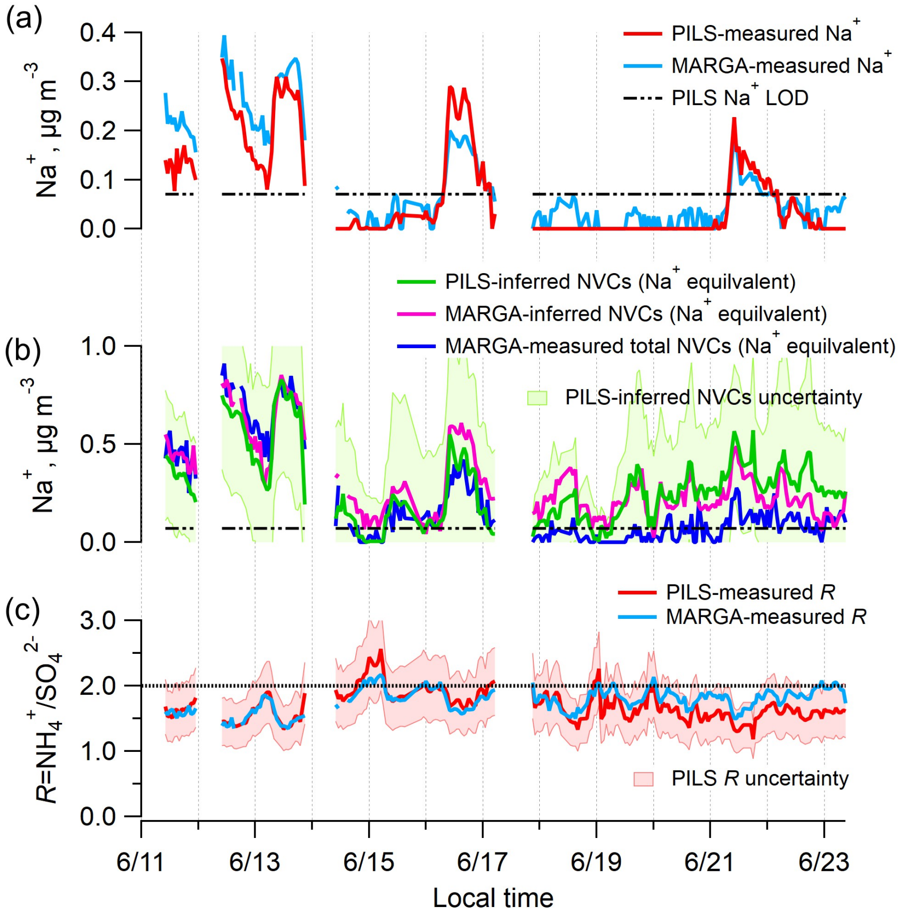

Fig. S2. (a) Comparison of $PM_{2.5}$ PILS and MARGA Na^+. (b) Comparison of inferred NVCs (from ion charge balance; $Na^+ = 2SO_4^{2-} + NO_3^- + Cl^- - NH_4^+$, nmol m^{-3}) by PILS and MARGA to measured total NVCs by MARGA (represented by Na^+), and (c) comparison of PILS and MARGA ammonium-sulfate molar ratios (*R*). Data are from the SOAS study.

S4. Comparison of ion charge balance inferred Na^+ including H^+ versus excluding H^+

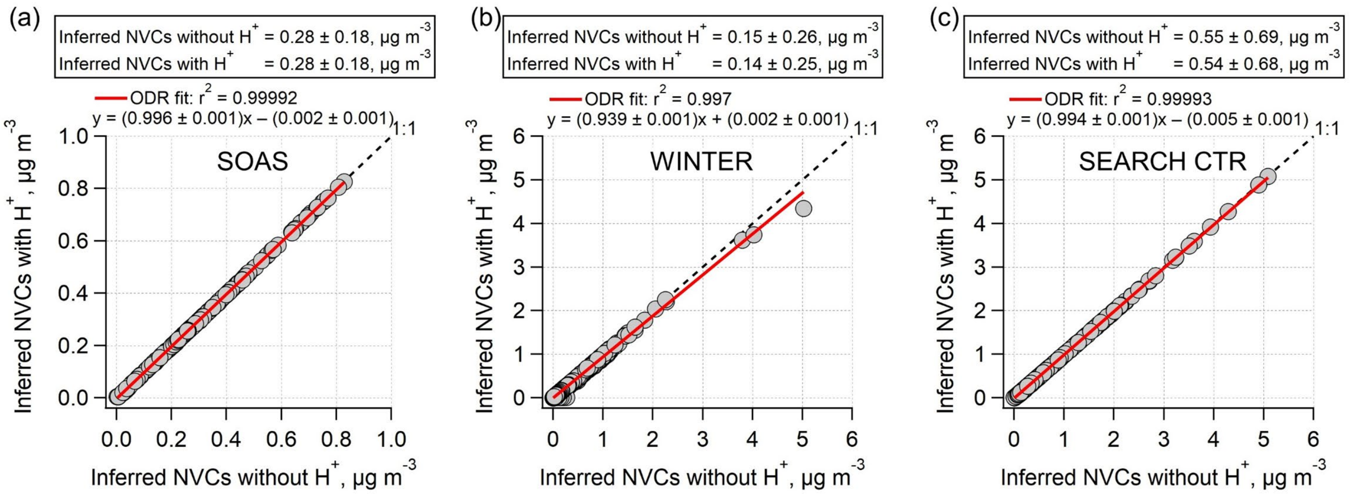

Fig. S3. Comparisons of ion charge balance inferred NVCs including H^+ ($Na^+ = 2SO_4^{2-} + NO_3^- + Cl^- - NH_4^+ - H^+$; y-axis) versus excluding H^+ ($Na^+ = 2SO_4^{2-} + NO_3^- + Cl^- - NH_4^+$; x-axis) for three data sets used in the paper, (a) SOAS (Fig. 1), (b) WINTER (Fig. 5), and (c) SEARCH CTR (Fig. 6). The H^+ concentration was determined using ISORROPIA in an iterative approach. Inferred NVCs were included with all other gas/particle species in the model, resulting in a predicted H^+. This H^+ is included in the ion balance to predict a new Na^+, which is then used in a new model iteration. The procedure is repeated until the Na^+ concentration converges. The number of iterations for conversion are 1 for (a), 5 for (b), and 0 for (c), respectively, until inferred NVCs converge. Orthogonal distance regression (ODR) fits are shown and uncertainties in the fits are one SD.

S5. Comparison of measured and ISORROPIA-predicted ammonium-sulfate molar ratios.

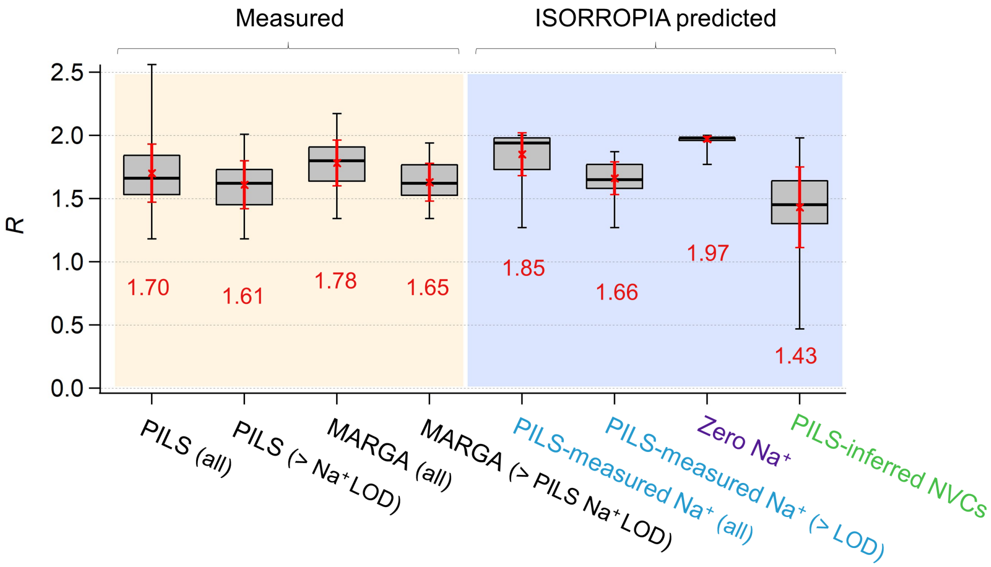

Fig. S4. Comparisons of $PM_{2.5}$ ammonium-sulfate molar ratios (R) between measurements and ISORROPIA predictions for the base case but with differing Na^+ inputs. Data are from the SOAS study. Red numbers are the means and red error bars are one SD. Standard box-whisker plots are shown, with 100% and 0% data indicated by black error bars. Top and bottom of box are the interquartile ranges (75% and 25%) centered around the median value (50%). Comparisons contrast all data and periods when measured Na^+ > PILS LOD of 0.07 μg m^{-3}. Inferred Na^+ is the value calculated from an ion charge balance representing NVCs.

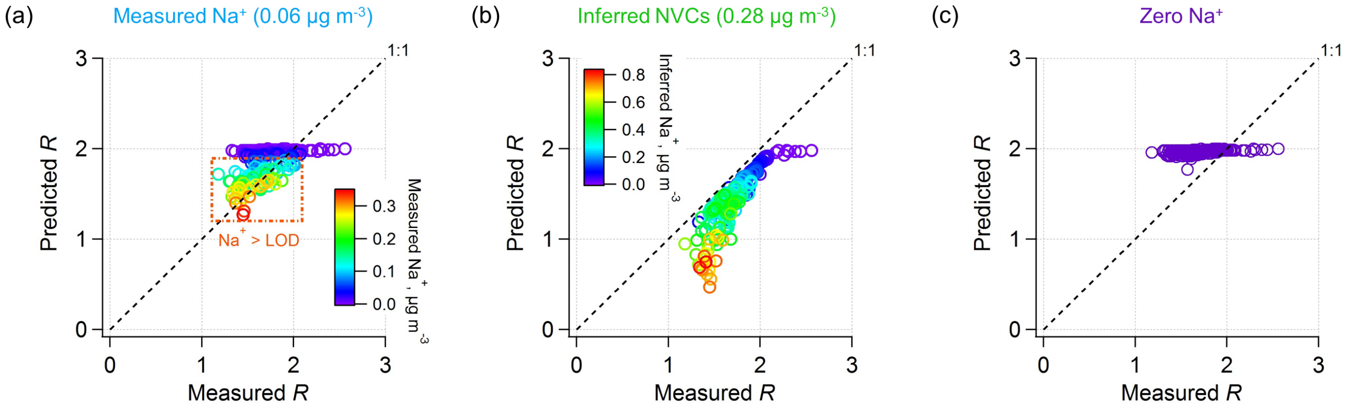

Fig. S5. Comparisons of $PM_{2.5}$ ammonium-sulfate molar ratios (R) between measurements and ISORROPIA predictions for differing Na^+ inputs for SOAS data. ISORROPIA was run with base case inputs and differing Na^+ inputs: (a) all Na^+ measured by the PILS, (b) NVCs (represented by Na^+) inferred from an ion balance, and (c) Na^+ set to zero.

S6. The relationships between errors in molar ratio and organic aerosol mass

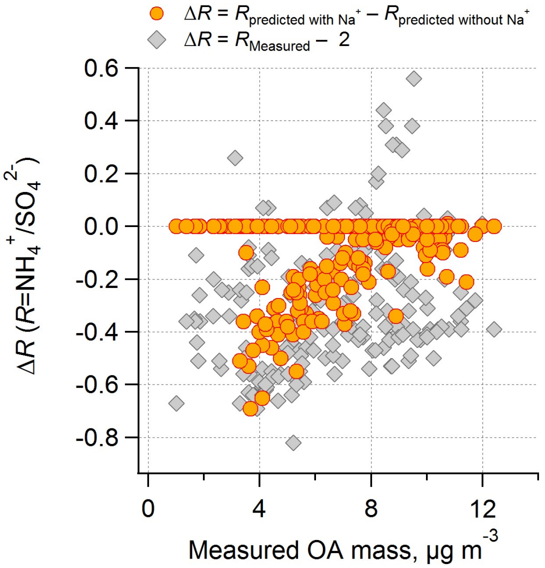

Fig. S6. Effect of nonvolatile cations (NVC) on the $PM_{2.5}$ ammonium-sulfate molar ratio (R) as a function of measured organic aerosol (OA) concentrations based on AMS data (SOAS). The orange circular points denote ΔR calculated from ISORROPIA-predicted R with measured Na^+ included in the model input minus ISORROPIA-predicted R without Na^+ in the model input. Grey diamonds are for ΔR equal to measured R minus 2. Note that ΔR should be negative since including Na^+ in the thermodynamic model results in R lower than 2, whereas not including Na^+ results in an R close to 2 (on average R predicted without Na^+ is 1.97 ± 0.02).

S7. Comparison of predicted and measured R_{SO4} by adding NVC

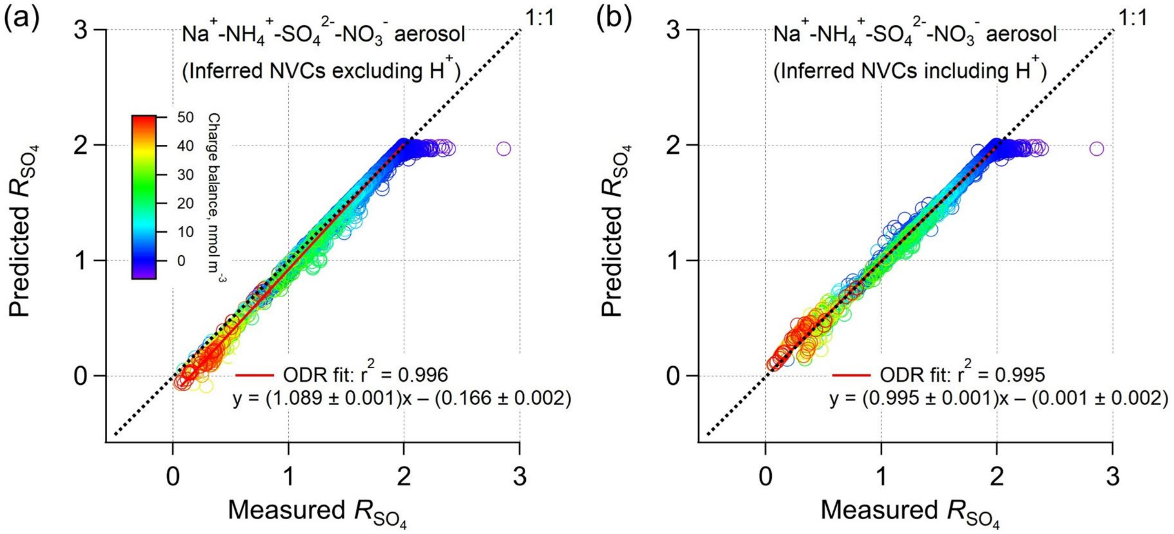

Fig. S7. Comparison between PM_1 AMS-measured R_{SO4} and ISORROPIA-predicted R_{SO4}, which is based on (a) inferred Na^+ excluding H^+ (see Fig. S3 x-axis) and (b) inferred Na^+ including H^+ (see Fig. S3 y-axis). The color wave indicates an ion charge balance, ($2SO_4^{2-} + NO_3^- - NH_4^+$) in units of nmol m^{-3}. The figure (a) is the same as Fig. 5b in the main text. The two results, (a) and (b) are very close, and the inferred Na^+ including H^+ produces slightly better result for a closer slope to one. ODR fits are shown and uncertainties in the fits are one SD.

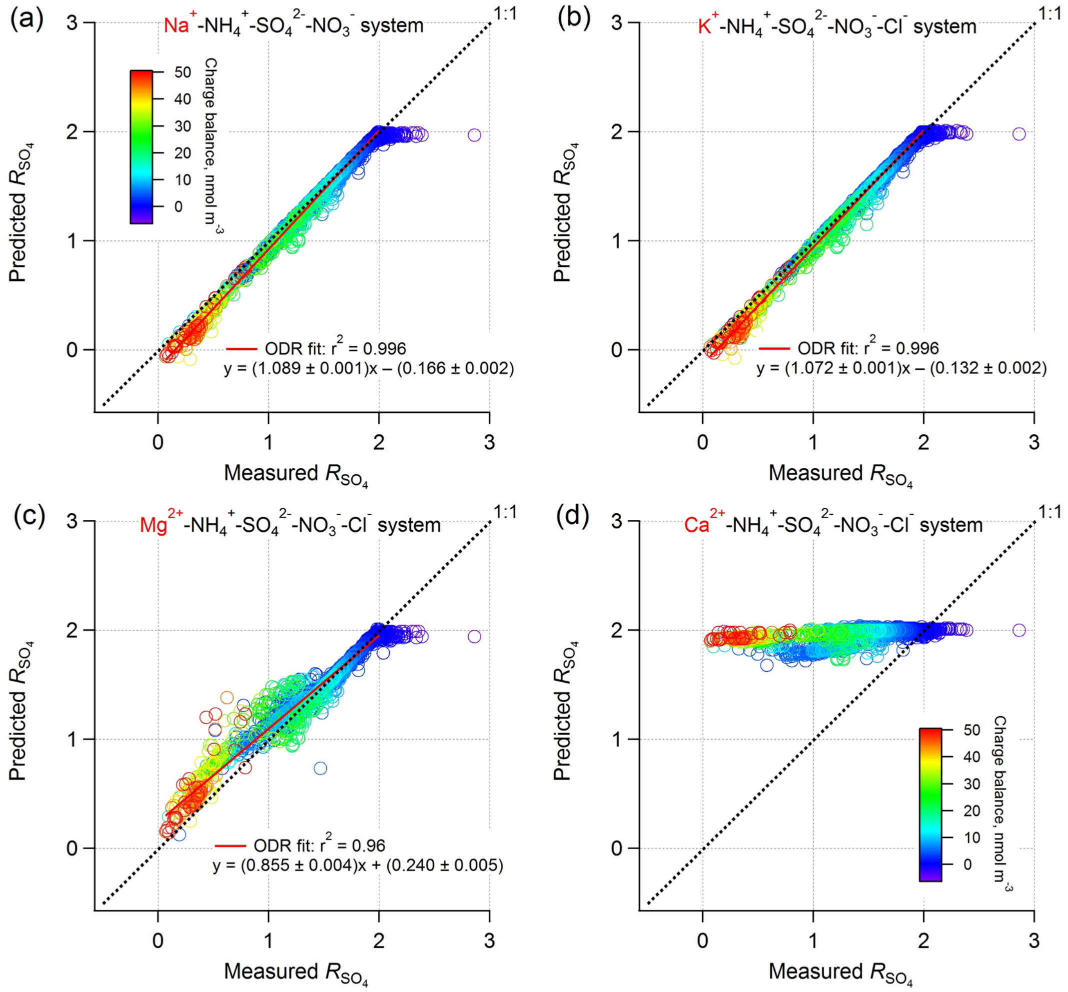

Fig. S8. Comparison between AMS-measured and ISORROPIA-predicted PM_1 R_{SO4} ($R_{SO4} = (NH_4^+ - NO_3^-)/SO_4^{2-}$, mol mol^{-1}), where the model predictions are based on NVC-NH_4^+-SO_4^{2-}-NO_3^-(-Cl^-) system for the WINTER study. NVC (nonvolatile cation) was determined by an ion charge balance (color wave), that is, ($2SO_4^{2-} + NO_3^- - NH_4^+$) in units of nmol m^{-3}. This results in 200% mole-equivalent concentrations of Na^+ and K^+ compared to Ca^{2+} and Mg^{2+} due to +1 versus +2 charges. NH_4^+, SO_4^{2-}, NO_3^- are observed AMS mass concentrations. For each graph, NVC is set to be a single species, including (a) Na^+, (b) K^+, (c) Ca^{2+}, (d) Mg^{2+}. For K^+, Ca^{2+}, and Mg^{2+}, a trace amount of total chloride (0.01 µg m^{-3}; a negligible level of Cl^-, 0.0012 µg m^{-3}, is predicted) is assumed to eliminate potential model errors but doesn't perturb the calculation of pH or HNO_3-NO_3^- partitioning. (Note that, Cl^- is only utilized as an input to ISORROPIA and is not included in the charge balance calculation.) Adding Na^+ and K^+ results in predicted R_{SO4} agreeing with measured R_{SO4}. Mg^{2+} also results in closer agreement, although some points deviate. Ca^{2+} doesn't work at all as it precipitates out from the aqueous phase as $CaSO_4$. The solubility of $CaSO_4$ is only 0.2 g per 100 mL water at 20 °C. An approximate calculation on $CaSO_4$ solubility shows that the average predicted particle liquid water W_i (2.0 µg m^{-3}) could only dissolve 0.004 µg m^{-3} Ca^{2+}, a tenfold lower amount than the inferred Ca^{2+} of 0.13 µg m^{-3} from an ion charge calculation. ODR fits are shown and uncertainties in the fits are one SD.

S8. The nonlinear response of NH_3-NH_4^+ or HNO_3-NO_3^- partitioning to pH (S curve)

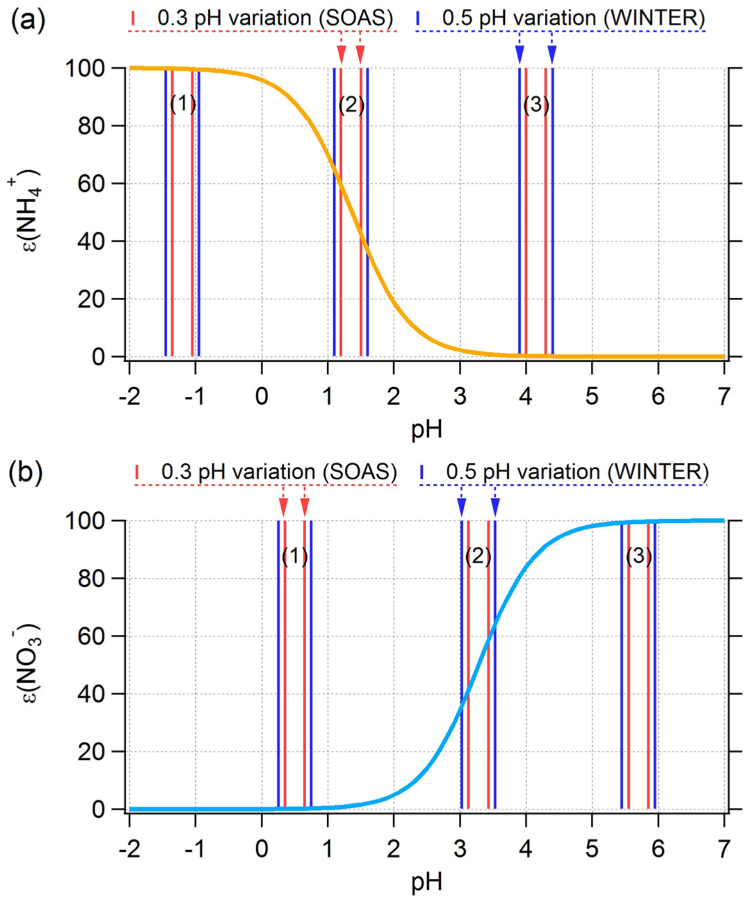

Fig. S9. S curves illustrate the nonlinear response in particle phase fraction, ε(NH_4^+) or ε(NO_3^-), to variation in pH: (a) ε(NH_4^+) and (b) ε(NO_3^-) plotted vs. pH. The two S curves are calculated based on T = 20 °C, particle liquid water level = 5 μg m^{-3}, and ideal solution (i.e. $\gamma = 1$). The S curve equations can be found at Guo et al. (2017). Non-ideality only shifts the S curves but does not change the shapes. The 0.3 unit pH (SOAS) and 0.5 unit pH (WINTER) variations (biases) are the upper limit values based on the difference between zero and inferred Na^+ inputs and indicated by paired red and blue sticks, respectively. The response of ε(NH_4^+) or ε(NO_3^-) to pH reaches maximum at 50% ε(NH_4^+) or ε(NO_3^-) (i.e., position (2), 0.3 unit pH change causes ~20% or 0.5 unit pH change causes ~30% shift in the particle phase fraction), but down to nearly zero when 100% or 0% ε(NH_4^+) or ε(NO_3^-) (e.g. position (1) or (3)).

S9. Thermodynamic predictions of the 15 years' summertime molar ratio at CTR site (Centreville, AL)

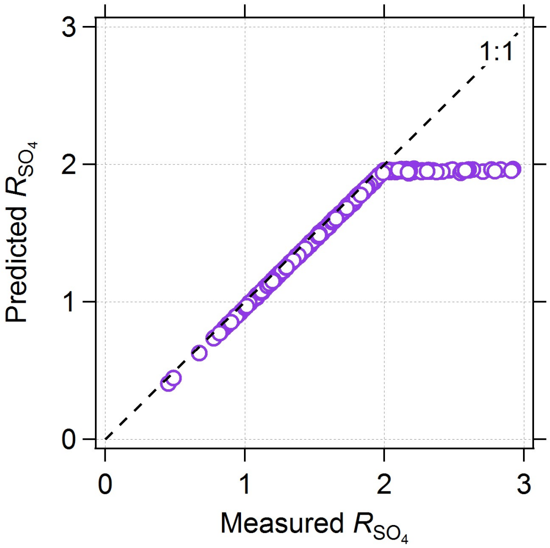

Fig. S10. Comparison of the measured and predicted R_{SO4} (with inferred Na^+ as input), summer means at CTR, as shown in the Figure 6 in the main text. The upper limit of R_{SO4} is 2 for a composition of $(NH_4)_2SO_4$ in ambient aerosols. A few observed points above 2 are results of measurement uncertainties.

S10. Internal vs. external mixture: the effect on molar ratio prediction

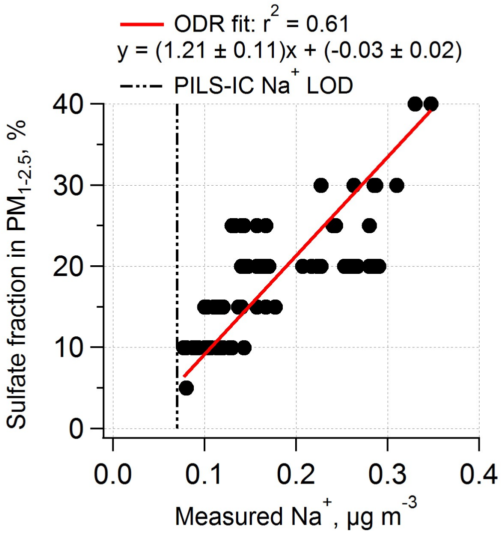

Fig. S11. Minimum sulfate fraction in $PM_{1-2.5}$ to obtain agreeable ammonium-sulfate molar ratio (*R*) between the internally and externally mixed aerosols (as shown in Fig. S9) versus measured Na^+ concentrations. This plot summarizes the results from Fig. S12.

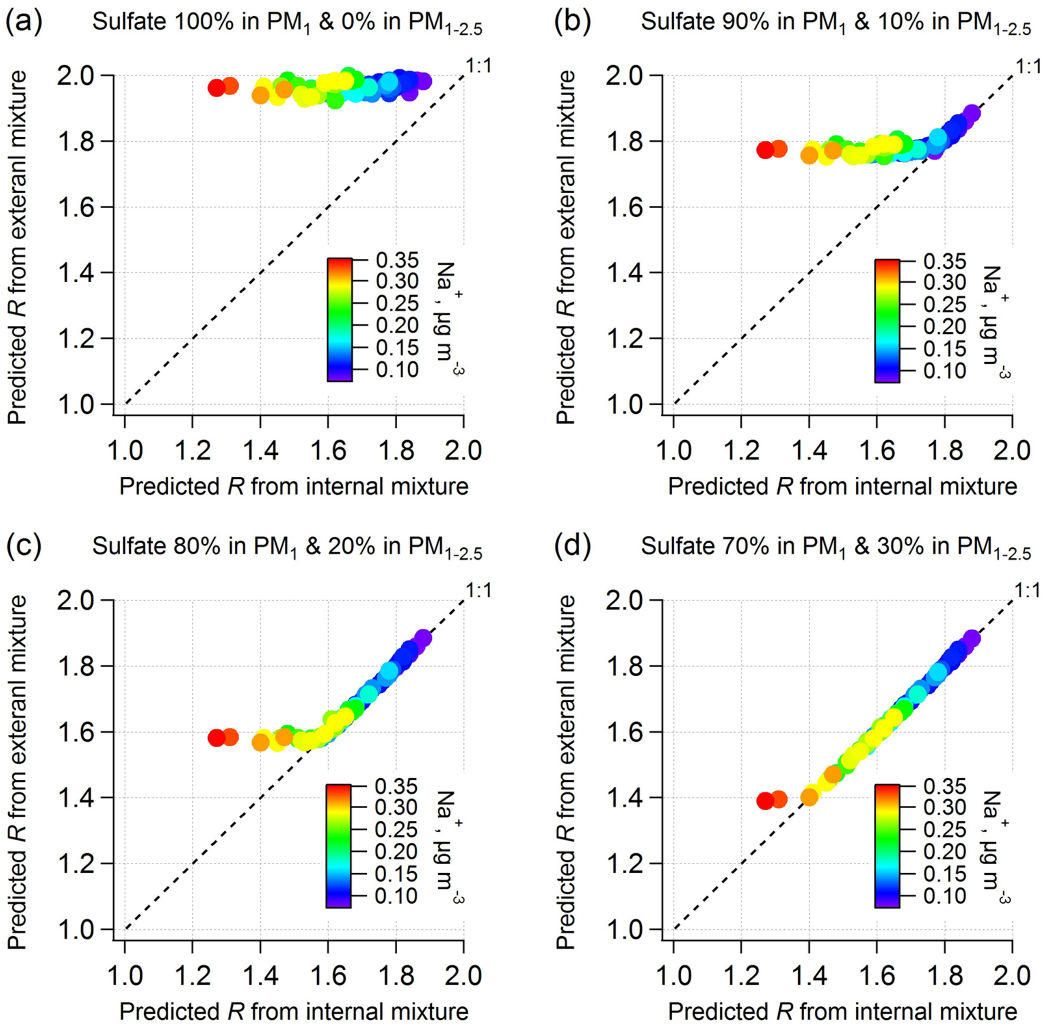

Fig. S12. Comparison of predicted *R* between internally and externally mixed aerosols, as shown in Figure 7 in the main text. NVCs (here represented by Na$^+$) are all assumed in PM$_{1-2.5}$ for the external mixing case, while (a) 0%, (b) 10%, (c) 20%, and (d) 30% (mass) fractions of PM$_{2.5}$ sulfate is assumed to be mixed with Na$^+$, as shown above each figure. The two points with the highest Na$^+$ concentrations require 40% sulfate in PM$_{1-2.5}$ to reach agreement (i.e. on 1:1 line).

References

Allen, H. M., Draper, D. C., Ayres, B. R., Ault, A., Bondy, A., Takahama, S., Modini, R. L., Baumann, K., Edgerton, E., Knote, C., Laskin, A., Wang, B., and Fry, J. L.: Influence of crustal dust and sea spray supermicron particle concentrations and acidity on inorganic NO_3^- aerosol during the 2013 Southern Oxidant and Aerosol Study, Atmos. Chem. Phys., 15, 10669-10685, doi: 10.5194/acp-15-10669-2015, 2015.

Edgerton, E. S., Hartsell, B. E., Saylor, R. D., Jansen, J. J., Hansen, D. A., and Hidy, G. M.: The Southeastern Aerosol Research and Characterization Study: Part II. Filter-Based Measurements of Fine and Coarse Particulate Matter Mass and Composition, J Air Waste Manan. Assoc., 55, 1527-1542, doi: 10.1080/10473289.2005.10464744, 2005.

Fountoukis, C., and Nenes, A.: ISORROPIA II: a computationally efficient thermodynamic equilibrium model for K^+-Ca^{2+}-Mg^{2+}-NH_4^+-Na^+-SO_4^{2-}-NO_3^--Cl^--H_2O aerosols, Atmos. Chem. Phys., 7, 4639-4659, doi: 10.5194/acp-7-4639-2007, 2007.

Guo, H., Xu, L., Bougiatioti, A., Cerully, K. M., Capps, S. L., Hite, J. R., Carlton, A. G., Lee, S. H., Bergin, M. H., Ng, N. L., Nenes, A., and Weber, R. J.: Fine-particle water and pH in the southeastern United States, Atmos. Chem. Phys., 15, 5211-5228, doi: 10.5194/acp-15-5211-2015, 2015.

Guo, H., Liu, J., Froyd, K. D., Roberts, J. M., Veres, P. R., Hayes, P. L., Jimenez, J. L., Nenes, A., and Weber, R. J.: Fine particle pH and gas–particle phase partitioning of inorganic species in Pasadena, California, during the 2010 CalNex campaign, Atmos. Chem. Phys., 17, 5703-5719, doi: 10.5194/acp-17-5703-2017, 2017.

Hidy, G. M., Blanchard, C. L., Baumann, K., Edgerton, E., Tanenbaum, S., Shaw, S., Knipping, E., Tombach, I., Jansen, J., and Walters, J.: Chemical climatology of the southeastern United States, 1999-2013, Atmos. Chem. Phys., 14, 11893-11914, doi: 10.5194/acp-14-11893-2014, 2014.

Solomon, P. A., Crumpler, D., Flanagan, J. B., Jayanty, R. K. M., Rickman, E. E., and McDade, C. E.: U.S. National $PM_{2.5}$ Chemical Speciation Monitoring Networks—CSN and IMPROVE: Description of networks, J Air Waste Manan. Assoc., 64, 1410-1438, doi: 10.1080/10962247.2014.956904, 2014.